Received: 24 August 2023 | Revised: 20 December 2023 | Accepted: 26 December 2023

https://doi.org/10.1016/j.jtha.2023.12.038

ORIGINAL ARTICLE

Thrombin activation of the factor XI dimer is a multistaged process for each subunit

Awital Bar Barroeta[1,2] | Pascal Albanese[3,4] | Tereza Kadavá[3,4] | Andris Jankevics[3,4,5] | J. Arnoud Marquart[1] | Joost C. M. Meijers[1,2,6] | Richard A. Scheltema[3,4,7]

[1]Department of Molecular Hematology, Sanquin, Amsterdam, the Netherlands

[2]Amsterdam Cardiovascular Sciences, Pulmonary Hypertension and Thrombosis, Amsterdam, the Netherlands

[3]Biomolecular Mass Spectrometry and Proteomics, Bijvoet Center for Biomolecular Research and Utrecht Institute for Pharmaceutical Sciences, Utrecht University, Utrecht, The Netherlands

[4]Netherlands Proteomics Centre, Utrecht, The Netherlands

[5]Univ. Grenoble Alpes, CNRS, INRAE, CEA, LPCV, INSERM, UMR BioSanté U1292, Grenoble, France

[6]Department of Experimental Vascular Medicine, Amsterdam UMC, University of Amsterdam, Amsterdam, the Netherlands

[7]Department of Biochemistry, Cell & Systems Biology, Institute of Systems, Molecular & Integrative Biology, University of Liverpool, Liverpool, UK

Correspondence
Joost C. M. Meijers, Dept. Experimental Vascular Medicine, Amsterdam UMC, Meibergdreef 9, 1105 AZ Amsterdam, the Netherlands.
Email: j.c.meijers@amsterdamumc.nl

Richard Scheltema, Biomolecular Mass Spectrometry and Proteomics, Padualaan 8, 3584 CH Utrecht, the Netherlands.
Email: r.a.scheltema@uu.nl

Abstract

Background: Factor (F)XI can be activated by proteases, including thrombin and FXIIa. The interactions of these enzymes with FXI are transient in nature and therefore difficult to study.

Objectives: To identify the binding interface between thrombin and FXI and understand the dynamics underlying FXI activation.

Methods: Crosslinking mass spectrometry was used to localize the binding interface of thrombin on FXI. Molecular dynamics simulations were applied to investigate conformational changes enabling thrombin-mediated FXI activation after binding. The proposed trajectory of activation was examined with nanobody 1C10, which was previously shown to inhibit thrombin-mediated activation of FXI.

Results: We identified a binding interface of thrombin located on the light chain of FXI involving residue Pro520. After this initial interaction, FXI undergoes conformational changes driven by binding of thrombin to the apple 1 domain in a secondary step to allow migration toward the FXI cleavage site. The 1C10 binding site on the apple 1 domain supports this proposed trajectory of thrombin. We validated the results with known mutation sites on FXI. As Pro520 is conserved in prekallikrein (PK), we hypothesized and showed that thrombin can bind PK, even though it cannot activate PK.

Conclusion: Our investigations show that the activation of FXI is a multistaged procedure. Thrombin first binds to Pro520 in FXI; thereafter, it migrates toward the activation site by engaging the apple 1 domain. This detailed analysis of the interaction between thrombin and FXI paves a way for future interventions for bleeding or thrombosis.

Manuscript handled by: Alan Mast

Final decision: Alan mast, 28 December 2023

Awital Bar Barroeta and Pascal Albanese contributed equally to this study.

Joost C. M. Meijers and Richard A. Scheltema contributed equally to this study.

Funding information J.C.M.M. acknowledges that this research was supported by grant 1702 from the Landsteiner Foundation for Blood Research. R.A.S. acknowledges that this work is part of the research program NWO TA with project number 741.018.201, financed by the Dutch Research Council (NWO). R.A.S. further acknowledges funding through the European Union Horizon 2020 program INFRAIA project Epic-XS (Project 823839). P.A. acknowledges the Dutch National Supercomputer, supported by NWO, for the computational resources (grant agreement EINF-894).

KEYWORDS
factor XI, mass spectrometry, prekallikrein, thrombin, XL-MS

1 | INTRODUCTION

Factor (F)XI is a protein that participates in the intrinsic pathway of coagulation. In the original model of coagulation, FXI could only be activated by FXIIa in the intrinsic pathway [1–3]. However, it was shown that FXI can also be activated by thrombin, creating a positive feedback loop that functions to maintain clot formation and stability [4–10]. A deficiency of FXI is associated with a mild bleeding disorder, while high levels of FXI are risk factors for venous and arterial thrombosis. Currently, thrombin-mediated activation of FXI is considered important for hemostasis, while FXIIa-mediated FXI activation may contribute to thrombosis.

FXI is a dimer of identical monomers, each consisting of 4 homologous apple domains (heavy chain) at the N-terminus that form a planar base for the chymotrypsin-like catalytic domain (light chain) at the C-terminus (Figure 1A) [11]. The catalytic domain is formed by 2 β-barrels linked by a flexible loop and contains a serine-based catalytic triad. In the planar base, each apple domain is structured into an antiparallel β-sheet of 7 β-strands that is curved around an α helix [11]. The apple domains are known to mediate the interactions between FXI and other proteins or charged surfaces. Moreover, the apple 4 domain mediates the covalent assembly of a homodimer through a disulfide bridge between the Cys321 residues of the 2 monomers [11–13]. FXI is activated through cleavage of the Arg369-Ile370 bond in the activation loop between the apple 4 domain and catalytic domain [11,12,14]. Initially, only 1 monomer is activated, generating a 1/2-FXIa intermediate that is functional and can activate FIX. The second subunit is activated in the second stage to obtain FXIa [15].

The interaction between FXI and thrombin is transient and difficult to study. This is exacerbated by the slow conversion rate of FXI when activated by thrombin, further complicating its characterization [4,8,10,16,17]. Nevertheless, peptide studies have proposed that thrombin interacts with the Ala45-Ser86 region in the apple 1 domain of FXI [18]. The enzymatic nature of the interaction implies a short-lived interplay between the proteins. In order to study such an interaction, it is ideally stabilized by covalent bonds between the 2 protein structures. Crosslinking reagents—small and agile chemicals covalently connecting amino acids in close proximity—have been developed precisely for this purpose, and when combined with mass spectrometry (termed crosslinking mass spectrometry [XL-MS]), they assist in the extraction of structural information for the proteins and their interactions [19]. After the crosslinking step, the sample is reduced, alkylated, and digested, yielding 3 distinct peptide products. Of these, the crosslinked peptide pairs are structurally informative upon identification of the peptide sequences. From these sequences, the locations within the protein structures can be derived, yielding information within 1 protein (both peptides from the same protein; intralinks) or between 2 proteins (peptides from different proteins; interlinks). The interlinks can be used, for example, to define the interaction interface between the 2 proteins and to even model the protein complex *in silico* [20], followed by molecular dynamics (MD) to study the behavior of the complex in solution [21]. Ultimately, the spacer length between the 2 reactive groups in the crosslinking reagent determines the maximum distance that can be bridged between lysine residues [22], which results in a resolution of 20 to 30 Å for this technique. However, detection of the low-abundant crosslinked peptide pairs is a challenge as they are present in a large background of unmodified peptides. To resolve this, enrichment handles were directly incorporated into the crosslinking reagents. One such reagent, termed PhoX, incorporates a small phosphonic acid in the spacer region that enables enrichment of crosslinked peptides using immobilized metal affinity chromatography [23]. With this efficient approach, the detection of crosslinked peptide pairs becomes readily feasible as the majority of the background is removed.

In this study, we report the interaction dynamics between FXI and thrombin *in vitro* and *in silico*. We found that the activation speed is sensitive to salt concentrations and is fastest at 50 mM, while it is almost completely stagnant at 150 mM NaCl. The reduced speed of activation at high salt conditions is likely advantageous for detecting the interaction with crosslinking reagents given that the crosslinking reagent takes minutes to complete; as we successfully capture the interaction the proteins are likely frozen into place for a longer period. Additionally, we localize thrombin on the catalytic domain (light chain) of FXI and further use the resulting distance constraints from XL-MS to construct an initial model of the full complex. This, however, places thrombin far from the cleavage site, excluding direct activation of FXI. To investigate how this is accomplished, we employed MD simulations, from which we were able to show that after the initial binding step,

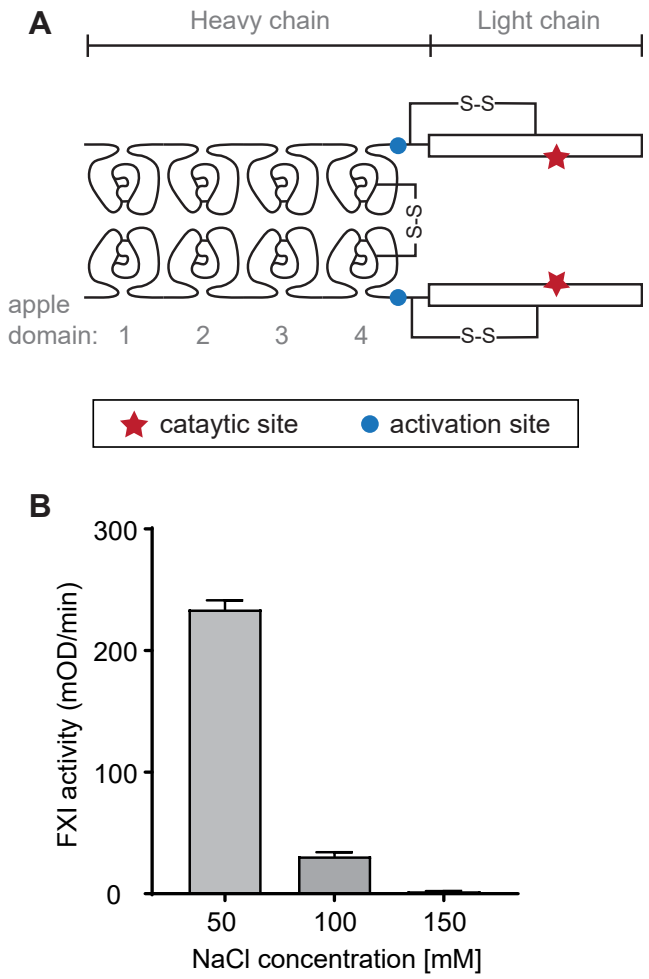

FIGURE 1 Interaction between factor (F)XI and thrombin. (A) Schematic model of FXI. (B) Salt concentrations affect FXI activation by thrombin. FXI activation was monitored in a buffer containing 50 mM, 100 mM, or 150 mM NaCl.

thrombin engages with the previously reported apple 1 domain and 2 amino acids on FXI, for which mutations exist that are known to lead to reduced activity. The trajectory of thrombin proposed by the MD simulations is further supported by competition studies of FXI-thrombin binding with anti-apple 1 nanobody 1C10 and prekallikrein (PK).

2 | MATERIALS AND METHODS

2.1 | FXI-WT and FXI-S557A production

FXI wild type (FXI-WT) with Cys11 replaced by Ser and FXI-S557A were prepared, as described previously [24]. The purified proteins were dialyzed against 10 mM 4-(2-hydroxyethyl)-1-piperazineethanesulfonic acid (HEPES), pH 7.5, containing 0.5 M NaCl, and stored at −80 °C until further use. The concentration of recombinant protein was determined by measuring the absorbance at 280 nm using the extinction coefficient for FXI (13.4).

2.2 | FII-S568A production

FII-WT cDNA with Ser568 (preprothrombin numbering, Ser525 in prothrombin numbering, and Ser195 in chymotrypsin numbering) replaced by Ala was produced, as reported previously [25]. Purified protein was dialyzed against 10 mM HEPES, pH 7.5, containing 0.6 M NaCl, and stored at −80 °C. The concentration of recombinant protein was determined by measuring the absorbance at 280 nm using the extinction coefficient for FII (13.6).

2.3 | FII-S568A activation

Activation of FII-S568A was performed, as described previously [25]. Purified protein was dialyzed against 10 mM HEPES, pH 7.5, containing 0.15 M NaCl, and stored at −80 °C. Completion of FII-S568A activation was monitored with sodium dodecyl sulphate-polyacrylamide gel electrophoresis (SDS-PAGE) (4%-12% Bis-Tris gel at 200 V for 50 minutes in morpholinopropane sulfonic acid) under reducing and nonreducing conditions (Supplementary Figure 1).

2.4 | FXI activation by thrombin under varying NaCl concentrations

FXI-WT (30 nM) was incubated for 10 minutes at 37 °C in assay buffer (30 mM HEPES, pH 7.4, 1 mg/mL bovine serum albumin) containing varying concentrations of NaCl: 50, 100, or 150 mM. After the addition of thrombin (5 nM, a kind gift from the late Dr Walter Kisiel, Albuquerque), the mixture was incubated for 30 minutes before the addition of hirudin (1 μg/mL). The mixture was incubated for 5 minutes before adding S2366 (0.5 mM) and measuring absorbance (405 nm) for 10 minutes at 37 °C.

2.5 | PhoX concentration optimization

Freshly dissolved crosslinking reagent PhoX (50 mM in anhydrous dimethyl sulfoxide) was aliquoted in Eppendorf tubes and stored at −20 °C. FXI-S557A (5 μg, 3.46 μM, 0.3 mg/mL) and thrombin-S205A (2.3 μg, 3.45 μM, 0.13 mg/mL) were diluted in 20 mM HEPES buffer, pH 7.4, with 100 mM, 125 mM, or 150 mM NaCl. Samples were incubated for 30 minutes at 37 °C. A PhoX aliquot was slowly heated to room temperature prior to use. The protein mixture (18 μL) was crosslinked with a concentration range of 0.25 to 2 mM PhoX over 30 minutes at room temperature, after which the reaction (20 μL) was quenched with 2.2 μL Tris-HCl (50 mM, pH 7.5). The crosslinked samples were subjected to SDS-PAGE (4%-12% Bis-Tris gel at 200 V for 50 minutes in MOPS) under reducing and nonreducing conditions. The gel was stained with Imperial Protein stain for 1 hour and destained in water overnight.

2.6 | Extraction of structural information and modeling

To obtain structural information, we used the workflow as detailed in the study by Steigenberger et al. [23]. A complete overview of the steps is provided in Supplementary Methods (*Crosslinking and Sample Preparation*, *Liquid Chromatography with Mass Spectrometry*, and *Data Analysis* sections).

Time-resolved investigation of the Cys321 mutant dimer [13,26] was performed with Refeyn OneMP. A complete overview is provided in FXI Cys321 mutant response to anions (Supplementary Methods).

All modeling was performed in ChimeraX [27,28], and the MD simulations were performed in Martini [29,30]. A complete overview of the steps is provided in Supplementary Methods (*Modeling of FXI dimer and docking of the thrombin binding to FXI* and *Molecular dynamics simulations* sections).

2.7 | Antibodies

A complete overview of the steps is provided in Supplementary Methods (*Generation of nanobodies targeting the apple 1 domain of FXI* and *Functional characterization of antiapple 1 nanobodies* sections).

2.8 | Fluorescence resonance energy transfer assay

Competition of PK (HPK393AL, Enzyme Research Laboratories) or nanobody 1C10 for thrombin binding to FXI was performed essentially as previously described [25] using a 20-hour incubation. Nanobody 2E4 was used as a negative control.

3 | RESULTS

3.1 | FXI activation by thrombin as a function of NaCl

The interaction interface between FXI and thrombin is not yet well defined [4,8,10,16,17], which can be attributed to the transient nature of the enzymatic reaction. Investigation into the buffer conditions showed that FXI activation speed is dependent on the salt concentrations in the assay buffer (Figure 1B). The activation speed was significantly enhanced in assay buffer containing 50 mM NaCl compared with 100 mM or 150 mM. Moreover, this was achieved after 10 minutes of incubation, while effective activation of FXI requires >72 hours of incubation in an assay buffer with 150 mM NaCl [17]. The longer activation time or prolonged interaction between the proteins, observed with 100 mM or 150 mM NaCl, is potentially advantageous for the following crosslinking step as this takes minutes to complete.

3.2 | Mapping of crosslinks on the FXI and thrombin protein structures

To elucidate the thrombin-binding epitope, we next applied crosslinking in buffers containing 100, 125, and 150 mM NaCl. These concentrations were selected to ensure that activation is still there, but at an extremely slow rate, which is more in line with the crosslinking reaction dynamics that take minutes to complete. This compromise ensures that crosslinks between the 2 subunits can form and structural data can be extracted. Crosslinking was observed for all tested crosslinker concentrations without overcrosslinking (Supplementary Figure S4). The different salt concentrations resulted in very similar profiles on the gel, although smearing of FXI for the lower salt concentrations is present, which is likely caused by improved accessibility of lysines to form monolinked products (one reactive group of the crosslinker reacted with a lysine, while the other quenched on Tris or H_2O). To remain on the conservative side, we performed further crosslinking experiments at the lower concentration of 0.3 mM PhoX. After filtering for at least 3 out of 4 replicate experiments, a total of 63 (intra: 61; inter: 2) for 100 mM, 74 (intra: 72; inter: 2) for 125 mM, and 76 (intra: 74; inter: 2) for 150 mM were identified from the acquired mass spectrometry data (representative annotated fragmentation spectra identifying the interlinks are provided in Supplementary Figure S5; all 33 annotated interlink spectra are provided in Supplementary File S2; Supplementary Table S1, tab Interlinks). The different salt concentrations gave reproducible identifications (Figure 2A), from which we conclude that all the selected salt concentrations result in a sufficiently slowed-down activation for the crosslinking reaction to capture the interaction (which is not expected to change location for different salt conditions). As expected, we detected the fewest links for 100 mM with increasing numbers for the higher salt concentrations. Going further, the data from all salt concentrations were used, especially as a unique interlink detected in the 100 mM dataset, bringing the total number of unique interlinks between FXI and thrombin to 3.

As quality control for the detected crosslinks, we mapped the intralinks on AlphaFold 2 structures of thrombin and FXI (Figure 2B). All links in thrombin and within the light and heavy chains of FXI fall well within the maximum distance constraint of 30 Å (Figure 2C). There was, however, a set of 30 intralinks that exceeded the maximum distance constraint. These intralinks were exclusively between the light and heavy chain of FXI and located around Lys183 and Lys248 on the heavy chain on the outer edge of the protein structure (Supplementary Figure S3A). As they are localized on the outer edge of FXI, it is very likely that these intralinks formed because the chains can reach each other through the flexible linker region connecting them. The existence of such conformations, induced by the flexible linker region, is well supported by reported electron microscopy data [31]. As this set of intralinks maps the flexible nature of the protein structure instead of the actual topology and will be difficult to interpret or use for structural modeling, it can be discarded from further analysis, and we conclude that our dataset accurately reflects the protein structure.

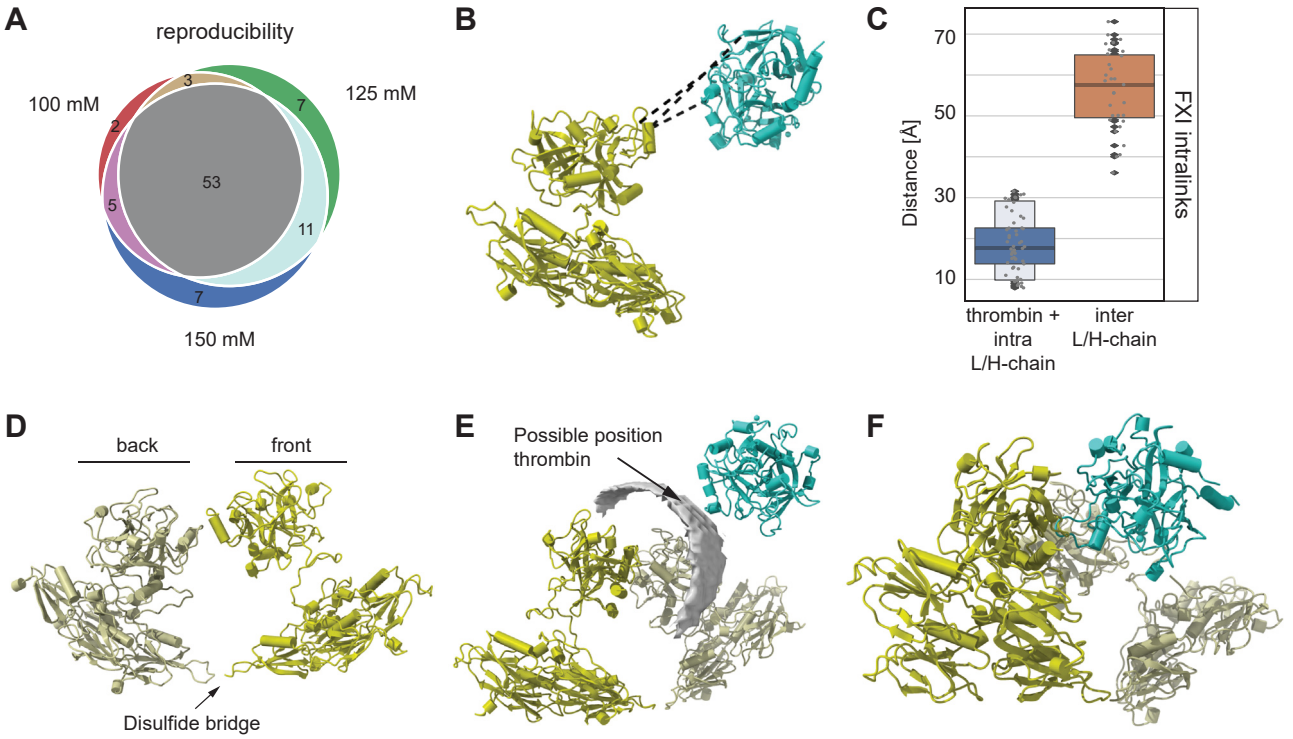

FIGURE 2 Crosslinking mass spectrometry results on factor (F)XI and thrombin. (A) Overlap of the detected crosslinks between the different salt concentrations. (B) The crosslinks (interlinks: black) mapped onto available AlphaFold 2 structural models in cartoon representation for FXI (AF-P03951-F1; forest green) and thrombin (AF-P00734-F1; sea green). (C) Validation of the crosslinks on FXI expressed as the measured distance inside the protein structure model. (D) Construction of the FXI dimer (monomer #1: forest green; monomer #2: light green). (E) Possible interaction interface between thrombin and FXI (grey density). (F) Final model of the FXI-thrombin complex.

3.3 | Constructing the complete model

A total of 2 self-links could be extracted from the crosslinking results. Such links are intralinks (ie, both peptides are from the same protein), but they are necessarily between 2 distinct copies of that protein and can be defined as interlinks, as described by Lagerwaard et al. [28]. We used these links together with the disulfide bridge at Cys321 to construct the dimer using the *in silico* structural modeling tool HADDOCK [32]. The resulting model places the 2 subunits mirrored to each other, which is the only possibility to satisfy the disulfide bridge and self-links and adjacently place the light chains (Figure 2D). Such a mirrored construction is likely as it automatically enables the previously reported 2-stepped activation procedure [15]. The final model slightly rotates the light chain of FXI compared with the crystal structure (Supplementary Figure S3B). This is, however, well within the range of possibility for the flexible linker connecting the light and heavy chains.

To construct the final model of FXI interacting with thrombin, we used a set of computational structural modeling tools. First, we investigated the detected interlinks with DisVis [32]. Interlinks that do not agree with the majority can be excluded using this analysis, which in this case were none. Additionally, the center of mass of thrombin relative to FXI can be detected (Figure 2E; grey density). From this, it is clear that thrombin can interact with the FXI dimer on both sides of the light chain. This was also expected, given the mirror construction of the homodimer that enables access from either side to one of the monomers. Next, we applied protein-protein docking by HADDOCK [32] to obtain the final model using the 3 interlinks. This resulted in a model where thrombin is located on the light chain of one monomer (Figure 2F). The location is surprising, however, as this places thrombin distal from the apple 1 domain on FXI, a domain that was previously reported as key for thrombin activation [18], as well as from the activation site.

3.4 | MD simulation

Our crosslinking results performed on a salt-induced frozen initial state of the interaction place thrombin on the light chain, which we hypothesized represents the initial (most stable) contact point for thrombin. Thrombin then needs to migrate toward the cleavage site to be able to activate FXI, which represents a highly dynamic process. To study the dynamics behind the FXI-thrombin interaction, we employed MD simulations. From the results, it can be observed that the structure of FXI first compresses (Figure 3A), after which thrombin migrates toward the cleavage site. At the start of this migration, thrombin engages the apple 1 domain of the FXI subunit (Figure 3B). This domain was previously reported as the key for thrombin binding via amino acids Ala45-Ser86 [18]. From the MD simulations, amino

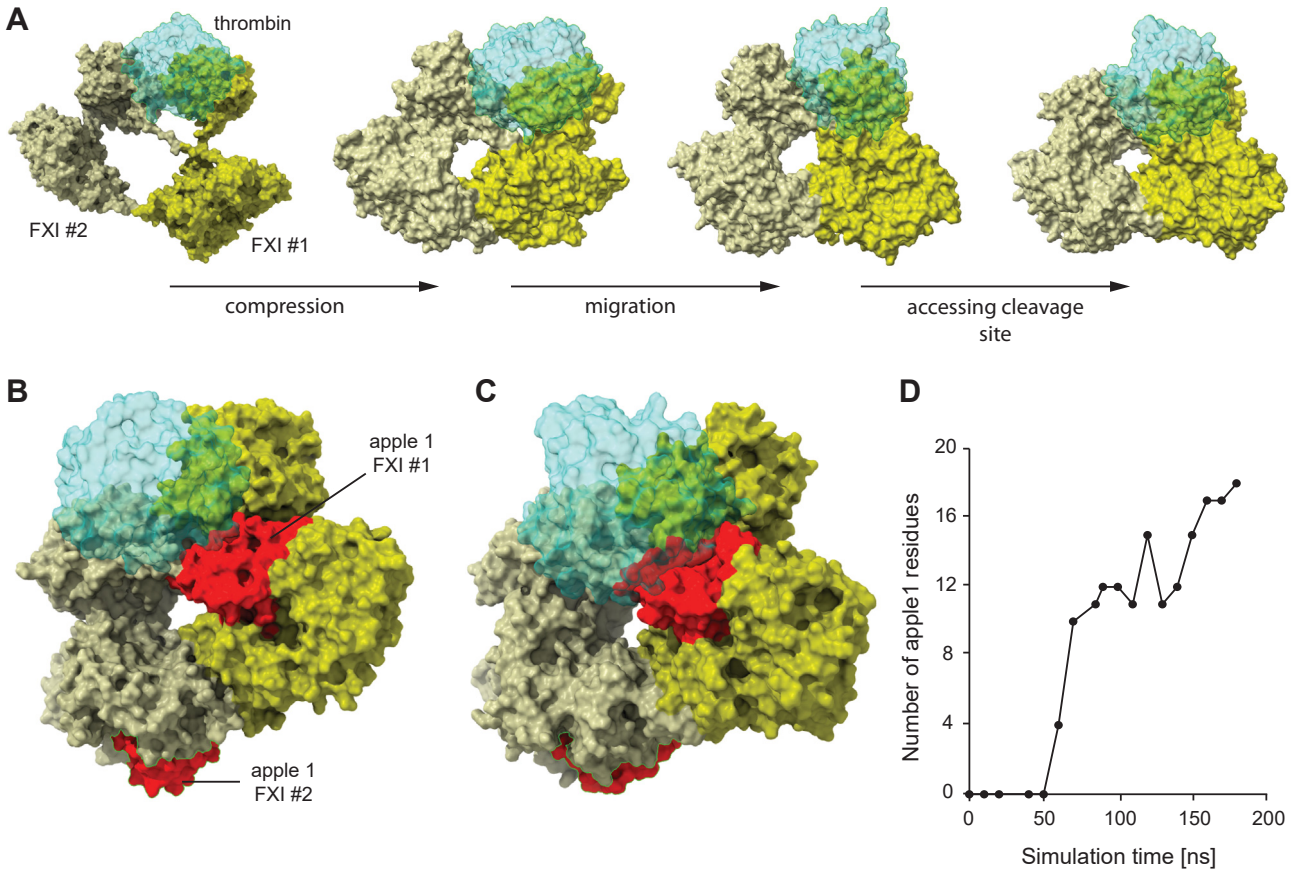

FIGURE 3 Molecular dynamics simulations. (A) Molecular dynamics simulation shows that upon binding, the factor (F)XI/thrombin complex undergoes 3 stages: compression, migration, and finally, cleavage site accession. (B) Engagement of the apple 1 domain at 60 ns in the simulation or during migration. (C) Increasingly more protein surface of FXI connected to thrombin at 180 ns. (D) Number of residues in the apple 1 domain contacting thrombin over a simulation time of 180 ns.

acids Ala45-Ile76 are highlighted as contacting as well as residues Cys2-Gln5. The N-terminal residues are near the others and also play a structural role. Based on these results, we conclude that apple 1 is important to initiate the migration of thrombin toward the cleavage site but not for the initial binding step. This is supported by the observation that more surface area of the apple 1 domain becomes engaged with thrombin over time (Figure 3C, D).

3.5 | Effect of naturally occurring mutations on FXI

A total of 185 mutations in FXI have previously been described (Supplementary Table S1; tab Mutations) [33–35]. The biggest fraction of these influence levels of FXI (n = 88) and the dimerization state of FXI (n = 9), which are not relevant for this study as they are unlikely to affect thrombin binding. The remaining fraction of mutations, however, may affect the activity or activation of FXI (n = 51) (Figure 4A). To further distinguish these mutations, we verified whether the mutated sites are shared with plasma PK, FXI's evolutionary predecessor (Supplementary Figure S6). This monomer homolog of FXI is not activated by thrombin [36], and therefore, shared mutation sites are potentially not involved in activation by thrombin. Of the 51 combined mutation sites that affect activity, 17 are unique for FXI (Figure 4A; inset). Mapping this set of mutations on the constructed dimer of FXI shows that the majority of the unique mutations (ie, not occurring in PK) are surface-exposed (13/17), pointing to a possible role in binding with thrombin, while the majority of the conserved mutations are inside the globular domain, pointing to a possible role in altering the structure of FXI's active site (Figure 4B, C). However, from the MD simulations, we observed that the migration of thrombin is a highly dynamic process that exposes and hides amino acids in the process and some of the conserved sites may still play a role. Following the interaction over time uncovers 2 residues (Figure 4D). The first, Pro520, is always in contact with thrombin. The second, Arg378, comes into play at a later stage in the process and appears to pull thrombin toward the cleavage site.

3.6 | Competition for the FXI-thrombin interaction with nanobody 1C10

The role of the apple 1 domain in the interaction between thrombin and FXI was further investigated with nanobody 1C10. This nanobody specifically targets the apple 1 domain, as confirmed with hydrogen-deuterium exchange mass spectrometry (see Materials and Methods). The hydrogen-deuterium exchange mass spectrometry illustrated that

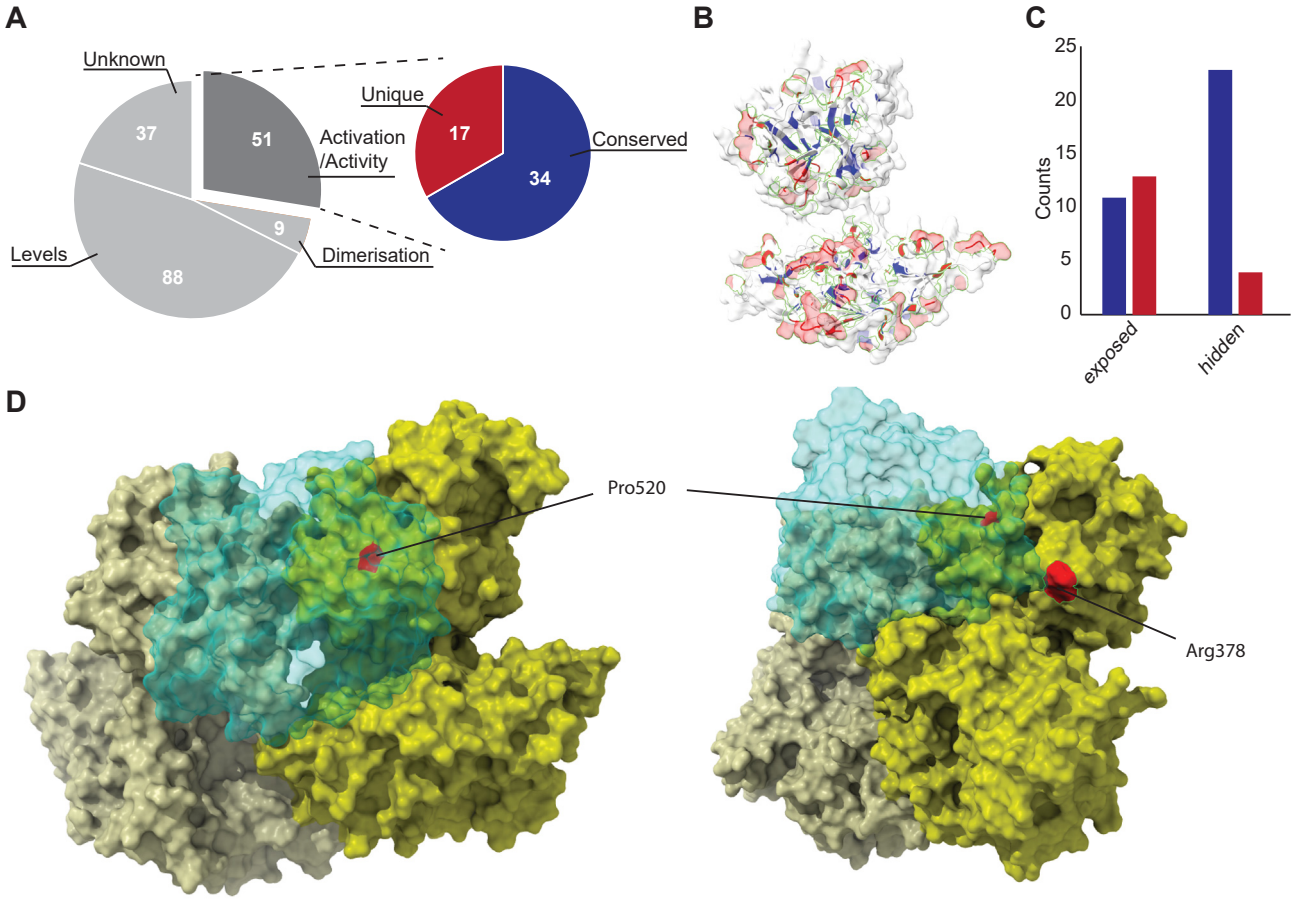

FIGURE 4 Mutations on factor (F)XI. (A) Effect of all known mutations. In the inset, a zoom-in on the mutations known to affect the activity of FXI separated in terms of whether the amino acids are conserved in prekallikrein (in blue) or unique for FXI (in red). (B) Mutations affecting activity mapped on FXI (same color scheme as in A). (C) Mutations affecting activity categorized in terms of whether they are surface exposed. (D) Molecular dynamics simulations uncovered Pro520 as important in binding (left; present always in the MD simulation) and Arg378 as important in migration (right; present after 130 ns of MD simulation time).

the binding epitope spans across peptide regions Val38-Val48 and Phe61-Phe77 (Figure 5A). Although this nanobody was able to interfere with the thrombin-mediated FXI activation in a dose-dependent manner (Figure 5B), it did not affect the binding between thrombin and FXI, as monitored with a fluorescence resonance energy transfer–based assay [25] (Figure 5C). This fits with the trajectory that we obtained in the MD simulations as the initial binding is far removed from the apple 1 domain and further highlights a secondary role for this domain in the interaction of thrombin with FXI that follows initial contact with the light chain. A control nanobody, 2E4, also directed against the apple 1 domain, neither influenced thrombin-mediated FXI activation (Figure 5B) nor FXI-thrombin binding (Figure 5C).

3.7 | Comparison of mutation sites with PK

Two of the naturally occurring mutation sites in FXI appeared to interact with thrombin in the MD simulation data and were further investigated. The first, Pro520, is present in PK but appears structurally important in binding thrombin as it remained in contact with thrombin at all time points of the MD simulation (Figure 3). This would indicate that PK may bind thrombin, even though it is not activated by it [36]. To verify whether this is possible, we performed molecular docking with HADDOCK of thrombin and PK based on the active residue Pro522 of PK. This indeed resulted in a credible model with no steric clashes (Figure 5D). We additionally confirmed that PK can interact with thrombin by demonstrating that it competes for thrombin binding to FXI (Figure 5E) using a fluorescence resonance energy transfer–based assay [25]. Given that the conserved proline is involved in the interaction with thrombin from the start of the simulation, binding to PK further supports that this amino acid is important for the initial binding of thrombin. Although PK also contains an apple 1 domain, it is not clear whether this domain can engage in thrombin binding as there are clear differences in the amino acid sequence. The second mutation site, Arg378, is not present in PK, pointing to a pivotal role in the actual activation.

3.8 | Subunit activation is a multistaged process

Based on the constructed models and MD simulations, a chain of events can be constructed, which finally leads to the activation of FXI.

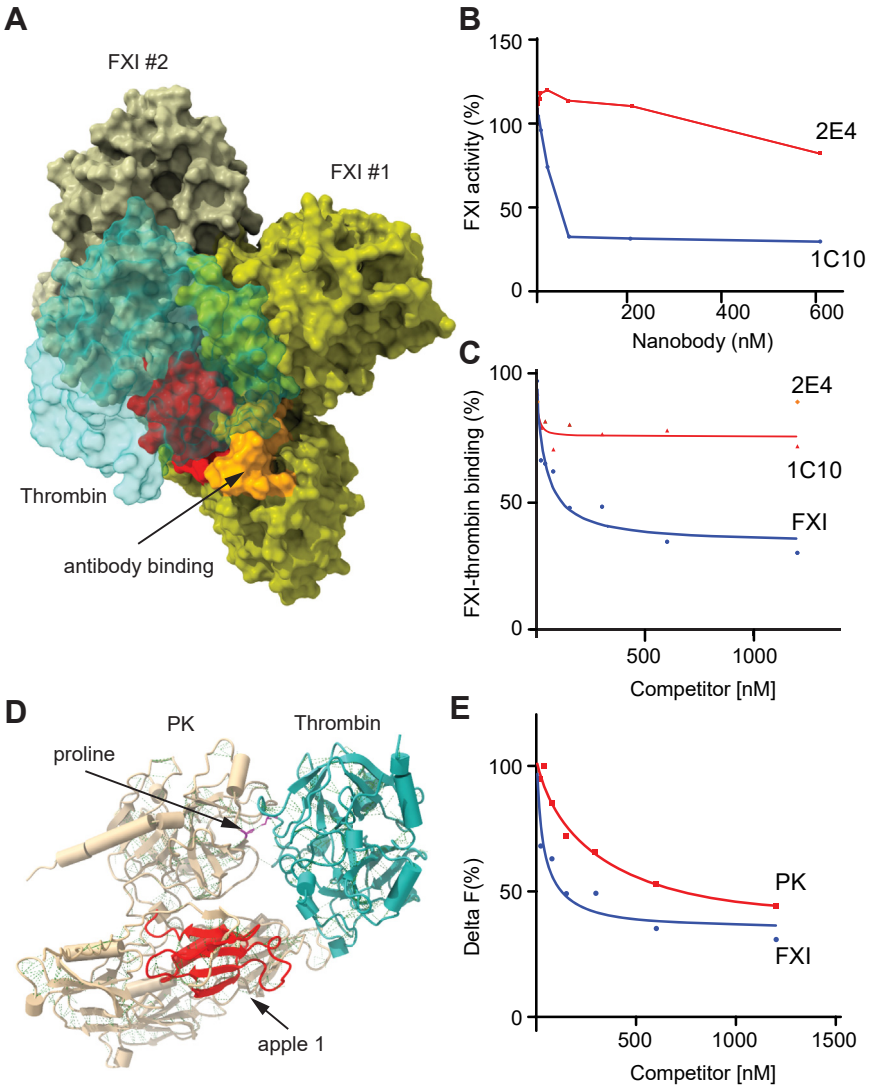

FIGURE 5 Competition of thrombin binding to factor (F)XI by PK and nanobody 1C10. (A) Epitope for antibody 1C10 (orange) on apple 1 (red) as determined by hydrogen-deuterium exchange mass spectrometry. (B) FXI activation by thrombin is dose-dependently competed by nanobody 1C10 and not by the control nanobody 2E4. (C) Nonlabelled FXI competes, while nanobodies 1C10 and 2E4 do not, for AlexaFluor647-labelled thrombin (300 nM) binding to Europium-labelled FXI (50 pM) in a fluorescence resonance energy transfer assay. (D) Molecular docking of thrombin and PK based on the residue Pro522. (E) Nonlabelled PK competes with binding between FXI and thrombin in the fluorescence resonance energy transfer assay. (B, C, E) Curves show results from a representative experiment (n = 3). PK, prekallikrein.

In the initial binding step, Pro520 is responsible for binding thrombin; then, the apple 1 domain starts to engage to migrate thrombin toward a location between the light and heavy chain, which is followed by locking of thrombin by Arg378 in place between the light and heavy chains. Once locked between these 2, thrombin can start to activate FXI.

4 | DISCUSSION

The binding site of thrombin in FXI has remained elusive due to the short-lived nature of the enzymatic interaction. Moreover, conversion to FXIa by thrombin is very inefficient, implying a poor interaction that obstructs proper characterization [4,8,10,16,17]. Little is therefore known about the interaction site of thrombin on FXI, but it has been proposed to span across Ala45-Ser86 in the apple 1 domain of FXI [18]. After binding, thrombin has to access the Arg369-Ile370 bond in the activation loop between the apple 4 domain and catalytic domain to activate FXI [11,12,14]. Here, we report the use of XL-MS and integrative modeling to elucidate the interaction of thrombin with FXI.

To aid the characterization of the FXI-thrombin interaction, we investigated conditions to influence FXI activation by thrombin. We observed that reducing the salt concentration significantly sped up the activation of FXI by thrombin. Higher salt concentrations potentially shield charged residues on the protein surface, thereby hindering electrostatic interactions between FXI and thrombin [37,38]. Although higher salt concentrations were reported to alter dimerization of the apple 4 domain and reduce dimer formation [39], dimerization did not differ greatly for the salt concentrations used in the crosslinking experiments [39]. To ensure the best likelihood of success for the XL-MS approach owing to the relatively slow speed of the crosslinking reaction, we selected the salt concentrations at the low end of speed of activation (100, 125, and 150 mM).

From the XL-MS results, a total of 53 crosslinks were detected in all sample conditions with excellent overlap for the higher salt concentrations where the activation is the slowest (100, 125, and 150 mM).

From the final set of crosslinks, a total of 2 self-links on FXI could be identified, which together with the known disulfide bridge on Cys321 allowed us to construct the FXI homodimer [11]. The 3 interlinks between FXI and thrombin allowed the construction of the full complex. Contrary to the crystal structure of the FXI dimer, in which the catalytic domains are located on either side of a central "tipi" structure formed by the 2 heavy chains [11], our model suggests that the catalytic domains face each other in the same vertical plane as the Cys321 disulfide bridge (Figure 2D). This conformation appears more compatible with the constitutive interaction between FXI and high-molecular weight kininogen (HK) in plasma [40,41]. HK binds the bottom plane of the apple 2 and apple 3 domains, which would sterically hinder the proximity of the heavy chain seen in the crystal structure. HK can be accommodated more readily in the model where the heavy chains lie on the same horizontal plane. HK was, however, not included in either the crystallization or the crosslinking experiments, and it would be interesting to see whether or how HK influences FXI conformation.

For the FXI dimer, we observe 2 points of interest in our model for the role of Cys321 in maintaining the dimer [13,42]. First, the light chains are connected through 3 hydrogen bonds (Supplementary Figure S7A). Interestingly, one of the bonds is coordinated between Arg532, Gly533, and His534. These amino acids form the anion binding site 2 that, when occupied by anions, accelerates thrombin-mediated activation [14]. Although it is thought that the presence of the anions enhances binding of thrombin, we posit that it is more likely that the repulsive force between the bound anions disrupts the other 2 hydrogen bonds. This will likely fully reveal the activation site on FXI, allowing thrombin to more easily cleave this site. Second, dimerization in apple 4 does not require the presence of the Cys321-mediated disulfide bridge, where Leu284, Ile290, and Tyr329 are thought to be the main remaining drivers [11,42]. Closer inspection of the FXI model reveals that these residues are involved in a β-sheet formation that maintains the loop that exposes Cys321 (Supplementary Figure S7B). This occupies these amino acids in hydrogen bonds, making it unlikely that they are the interaction sites. *In silico* mutation of these residues to Ala shows a dramatic effect on both the β-sheet structure and the loop, while the rest of apple 4 remains unaffected (Supplementary Figure S7B; inset). Taken together, this suggests that binding between apple 4 domains even in the absence of Cys321 is mediated by residues in the loop. To verify the role of anions in disrupting the salt bridges, we traced the decay of a mutant lacking the Cys residue over time. We observed that although this mutant dimerizes, the dimer is not stable over time. With the addition of a low concentration of anions, the dimer is somewhat stabilized, which is potentially caused by changes in the buffer. However, at higher concentrations, the decay is significantly sped up, suggesting that the anions are outcompeting the salt bridges (Supplementary Figure 7C, D).

The final FXI/thrombin complex model places thrombin on the light chain (Figure 2F). As this region is far removed from the activation loop, we investigated the FXI-thrombin interaction and a possible activation mechanism using MD. Based on this, we propose that FXI compresses after binding to thrombin, shortening the distance between the catalytic domain and the apple 1 domain. This allows the interaction of thrombin to the apple 1 domain, followed by thrombin moving along the heavy chain to reach the activation loop. Interestingly, this supports cis-activation (within one monomer) rather than the previously proposed trans-activation [11]. Our experimental data validated the interaction of thrombin with the apple 1 domain [18] and proposed an initial binding site of thrombin on the light chain of FXI.

To investigate the probability of the proposed activation mechanism of thrombin on FXI, we compared the trajectory of thrombin on FXI with mutations known to cause reduced activity of FXI in patients [33,34]. This highlighted 2 residues on FXI, where Pro520 is involved with early binding and Arg378 in further migrating thrombin after it engages with the apple 1 domain. Both these residues have known mutations that were shown to affect activation. Interestingly, Pro520 is present in PK, suggesting that thrombin can bind this enzyme, although it cannot activate it. Indeed, we were able to show that PK competes for binding of FXI (Figure 5E). Arg378 is unique to FXI, however, and likely represents a key step in the activation dynamics of FXI. Interestingly, no mutations are present on the binding interface of thrombin on the FXI apple 1 domain, which leads to reduced activity. This may point to an essential role of this interface in binding other enzymes as well. To confirm the results of our computational findings, the proposed binding interfaces should be investigated/verified with mutation studies. A precise understanding of the interaction of thrombin, but also FXIIa, with FXI may provide essential information to guide the development of novel antithrombotic or prohemostatic treatments.

ACKNOWLEDGMENTS

J.C.M.M. acknowledges that this research was supported by grant 1702 from the Landsteiner Foundation for Blood Research. R.A.S. acknowledges that this work is part of the research program NWO TA with project number 741.018.201, financed by the Dutch Research Council (NWO). R.A.S. further acknowledges funding through the European Union Horizon 2020 program INFRAIA project Epic-XS (Project 823839). P.A. acknowledges the Dutch National Supercomputer, supported by NWO, for the computational resources (grant agreement EINF-894).

AUTHOR CONTRIBUTIONS

R.A.S., P.A., and J.C.M.M. designed the study. A.B.B. and J.A.M. performed the experiments. P.A. performed the mass spectrometry data acquisition, data analysis, and the structural modeling (protein-protein docking and molecular dynamics simulations). T.K. and A.J. performed mass photometry experiments and analyzed respective data. R.A.S. analyzed the structural data. A.B.B., J.C.M.M., and R.A.S. wrote the manuscript with help from all authors.

DECLARATION OF COMPETING INTERESTS

There are no competing interests to disclose.

DATA AVAILABILITY

The mass spectrometry proteomics data have been deposited to the ProteomeXchange Consortium via the PRIDE partner repository with the dataset identifier PXD039489 (reviewer_pxd039489@ebi.ac.uk).

REFERENCES

[1] Davie EW, Ratnoff OD. Waterfall sequence for intrinsic blood clotting. *Science*. 1964;145:1310–2.

[2] Schmaier AH. The contact activation and kallikrein/kinin systems: pathophysiologic and physiologic activities. *J Thromb Haemost*. 2016;14:28–39.

[3] Mann KG. Thrombin formation. *Chest*. 2003;124:4S–10S.

[4] Kravtsov DV, Matafonov A, Tucker EI, Sun M, Walsh PN, Gruber A, Gailani D. Factor XI contributes to thrombin generation in the absence of factor XII. *Blood*. 2009;114:452–8.

[5] Gale AJ. Current understanding of hemostasis. *Toxicol Pathol*. 2011;39:273–80.

[6] Versteeg HH, Heemskerk JWMM, Levi M, Reitsma PH. New fundamentals in hemostasis. *Physiol Rev*. 2013;93:327–58.

[7] von dem Borne PAK, Meijers JCM, Bouma BN. Feedback activation of factor XI by thrombin in plasma results in additional formation of thrombin that protects fibrin clots from fibrinolysis. *Blood*. 1995;86:3035–42.

[8] Gailani D, Broze GJ. Factor XI activation in a revised model of blood coagulation. *Science*. 1991;253:909–12.

[9] Zucker M, Seligsohn U, Salomon O, Wolberg AS. Abnormal plasma clot structure and stability distinguish bleeding risk in patients with severe factor XI deficiency. *J Thromb Haemost*. 2014;12:1121–30.

[10] Matafonov A, Sarilla S, Sun MF, Sheehan JP, Serebrov VM, Verhamme IM, Gailani D. Activation of factor XI by products of prothrombin activation. *Blood*. 2011;118:437–45.

[11] Papagrigoriou E, McEwan PA, Walsh PN, Emsley J. Crystal structure of the factor XI zymogen reveals a pathway for transactivation. *Nat Struct Mol Biol*. 2006;13:557–8.

[12] McMullen BA, Fujikawa K, Davie EW. Location of the disulfide bonds in human coagulation factor XI: the presence of tandem apple domains. *Biochemistry*. 1991;30:2056–60.

[13] Meijers JCM, Mulvihill ER, Davie EW, Chung DW. Apple four in human blood coagulation factor XI mediates dimer formation. *Biochemistry*. 1992;31:4680–4.

[14] Mohammed BM, Matafonov A, Ivanov I, Sun M fu, Cheng Q, Dickeson SK, Li C, Sun D, Verhamme IM, Emsley J, Gailani D. An update on factor XI structure and function. *Thromb Res*. 2018;161:94–105.

[15] Smith SB, Verhamme IM, Sun M, Bock PE, Gailani D. Characterization of novel forms of coagulation factor Xia: independence of factor XIa subunits in factor IX activation. *J Biol Chem*. 2008;283:6696–705.

[16] Choi SH, Smith SA, Morrissey JH. Polyphosphate is a cofactor for the activation of factor XI by thrombin. *Blood*. 2011;118:6963–70.

[17] Stroo I, Marquart JA, Bakhtiari K, Plug T, Meijer AB, Meijers JCM. Chemical footprinting reveals conformational changes following activation of factor XI. *Thromb Haemost*. 2018;118:340–50.

[18] Baglia FA, Badellino KO, Ho DH, Dasari VR, Walsh PN. A binding site for the kringle II domain of prothrombin in the Apple 1 domain of factor XI. *J Biol Chem*. 2000;275:31954–62.

[19] Steigenberger B, Albanese P, Heck AJR, Scheltema RA. To cleave or not to cleave in XL-MS? *J Am Soc Mass Spectrom*. 2020;31:196–206.

[20] van Zundert GCP, Rodrigues JPGLM, Trellet M, Schmitz C, Kastritis PL, Karaca E, Melquiond ASJ, van Dijk M, de Vries SJ, Bonvin AMJJ. The HADDOCK2.2 web server: user-friendly integrative modeling of biomolecular complexes. *J Mol Biol Netherlands*. 2016;428:720–5.

[21] Hollingsworth SA, Dror RO. Molecular dynamics simulation for all. *Neuron*. 2018;99:1129–43.

[22] Belsom A, Rappsilber J. Anatomy of a crosslinker. *Curr Opin Chem Biol England*. 2021;60:39–46.

[23] Steigenberger B, Pieters RJ, Heck AJR, Scheltema RA. PhoX: an IMAC-enrichable cross-linking reagent. *ACS Cent Sci*. 2019;5:1514–22.

[24] Bar Barroeta A, van Galen J, Stroo I, Marquart JA, Meijer AB, Meijers JCM. Hydrogen-deuterium exchange mass spectrometry highlights conformational changes induced by factor XI activation and binding of factor IX to factor XIa. *J Thromb Haemost*. 2019;17:2047–55.

[25] Bar Barroeta A, Marquart JA, Meijers JCMM. A FRET-based assay for the quantitation of the thrombin-factor XI interaction. *Thromb Res*. 2022;214:23–8.

[26] Cheng Q, Sun MF, Kravtsov DV, Aktimur A, Gailani D. Factor XI apple domains and protein dimerization. *J Thromb Haemost*. 2003;1:2340–7.

[27] Pettersen EF, Goddard TD, Huang CC, Meng EC, Couch GS, Croll TI, Morris JH, Ferrin TE. UCSF ChimeraX: structure visualization for researchers, educators, and developers. *Protein Sci*. 2021;30:70–82.

[28] Lagerwaard IM, Albanese P, Jankevics A, Scheltema RA. Xlink Mapping and AnalySis (XMAS) - smooth integrative modeling in Preprint. Posted online June 29, 2022. bioRxiv 489026. https://doi.org/10.1101/2022.04.21.489026.

[29] Qi Y, Ingólfsson HI, Cheng X, Lee J, Marrink SJ, Im W. CHARMM-GUI martini maker for coarse-grained simulations with the martini force field. *J Chem Theor Comput*. 2015;11:4486–94.

[30] Wassenaar TA, Pluhackova K, Böckmann RA, Marrink SJ, Tieleman DP. Going backward: a flexible geometric approach to reverse transformation from coarse grained to atomistic models. *J Chem Theory Comput*. 2014;10:676–90.

[31] Wu W, Sinha D, Shikov S, Yip CK, Walz T, Billings PC, Lear JD, Walsh PN. Factor XI homodimer structure is essential for normal proteolytic activation by factor XIIa, thrombin, and factor XIa. *J Biol Chem*. 2008;283:18655–64.

[32] Honorato RV, Koukos PI, Jiménez-García B, Tsaregorodtsev A, Verlato M, Giachetti A, Rosato A, Bonvin AMJJ. Structural biology in the clouds: the WeNMR-EOSC ecosystem. *Front Mol Biosci*. 2021;8:729513.

[33] Saunders RE, O'Connell NM, Lee CA, Perry DJ, Perkins SJ. Factor XI deficiency database: an interactive web database of mutations, phenotypes, and structural analysis tools. *Hum Mutat*. 2005;26:192–8.

[34] Saunders RE, Shiltagh N, Gomez K, Mellars G, Cooper C, Perry DJ, Tuddenham EG, Perkins SJ. Structural analysis of eight novel and 112 previously reported missense mutations in the interactive FXI mutation database reveals new insight on FXI deficiency. *Thromb Haemost*. 2009;102:287–301.

[35] Harris VA, Lin W, Perkins SJ. Analysis of 272 genetic variants in the upgraded interactive FXI web database reveals new insights into FXI deficiency. *TH Open*. 2021;05:e543–56.

[36] Ponczek MB, Shamanaev A, LaPlace A, Dickeson SK, Srivastava P, Sun MF, Gruber A, Kastrup C, Emsley J, Gailani D. The evolution of factor XI and the kallikrein-kinin system. *Blood Adv*. 2020;4:6135–47.

[37] Voznesensky AI, Schenkman JB. Quantitative analyses of electrostatic interactions between NADPH- cytochrome P450 reductase and cytochrome P450 enzymes. *J Biol Chem*. 1994;269:15724–31.

[38] McCoy AJ, Chandana Epa V, Colman PM. Electrostatic complementarity at protein/protein interfaces. *J Mol Biol*. 1997;268:570–84.

[39] Dorfman R, Walsh PN. Noncovalent interactions of the apple 4 domain that mediate coagulation factor XI homodimerization. *J Biol Chem*. 2001;276:6429–38.

[40] Thompson R, Mandle RJ, Kaplan AP. Studies of binding of prekallikrein and factor XI to high molecular weight kininogen and its light chain. *Proc Natl Acad Sci U S A*. 1979;76:4862–6.

[41] Thompson RE, Mandle R, Kaplan AP. Association of factor XI and high molecular weight kininogen in human plasma. *J Clin Invest*. 1977;60:1376–80.

[42] Zucker M, Zivelin A, Landau M, Rosenberg N, Seligsohn U. Three residues at the interface of factor XI (FXI) monomers augment covalent dimerization of FXI. *J Thromb Haemost*. 2009;7:970–5.

SUPPLEMENTARY MATERIAL

The online version contains supplementary material available at https://doi.org/10.1016/j.jtha.2023.12.038